Paramagnetic Resonance in Copper Acetate Monohydrate

Hidetaro Abe (阿 部 英 太 郎)
Department of Physics, Faculty of Science,
Ochanomizu University, Tokyo
and
Junji Shimada (島 田 順 二)
Institute of Science and Technology,
University of Tokyo, Tokyo

Abstract

Copper acetate monohydrate $Cu(CH_3COO)_2 \cdot H_2O$ was examined in its single crystals by paramagnetic resonance method using microwaves of 4 different wavelengths ($\lambda = 8 \sim 31$ mm). The spectra obtained are anomalous to be explained by the usual crystalline field theory applied to a Cu^{++} ion $(3d)^9$, in ^2D state. They can be explained by a spin-Hamiltonian with an effective spin $S=1$ which is originated from a pair of Cu^{++} ions coupled strongly in each other.

This cluster model with pairs of Cu^{++} ions agrees well with the result of x-ray analysis which shows afterwards the unit cell consists of constituents $Cu_2(CH_3COO)_4 \cdot 2H_2O$ and copper atoms in this unit approach as close as 2.64 Å each other.

§ 1. Introduction

In 1951, we had a plan of researches with method of paramagnetic resonance absorption to examine copper salts derived from the series of monocarboxylic acids; copper formate, copper acetate, copper propionate and so on. Then we started to make grow their single crystals.

We obtained, at first, single crystals of the copper acetate monohydrate $Cu(CH_3COO)_2 \cdot H_2O$, so we put them under examination. The observation was done at room temperature using our standard apparatus of 16 mm wavelength which was just under running state at that time. The spectrum obtained was not normal as those shown by Cu^{++} ions in ordinary hydrated crystals as in the copper Tutton salts and in the copper sulfate. So we repeated, at one hand, our experiments from the beginning of preparing the sample reagent with row materials supplied from another source, and on the other hand, we discussed this result with researchers of theoretical side.

In the meantime, Kambe gave an explanation[1] to this spectrum with a model of clusters of two strongly coupled Cu^{++} ions. It was thought that the origin of this anomalous spectrum becomes very interesting one, if the interaction between the two Cu^{++} ions in a couple is very strong compared with the other interactions from ions belonging to the other couples as a result of a super-exchange type coupling,

while all the Cu–Cu distances are ordinary ones, of order 5Å. So the x-ray analysis of this salt was eagerly desired.

After then, we knew that Lancaster and Gordy[2] examined this salt in powder form. They reported that there are anomalies in the spectrum of this salt which can not be explained by application of the ordinary crystalline field theory to the ^2D ground state of Cu^{++} ions. Moreover, they suggested that a line appeared near the half of the resonance field for normal copper salts could be explained through interaction between neighbouring copper ions.

On the other hand, Bleaney and Bowers at Clarendon Laboratory have also begun to examine this salt with paramagnetic resonance absorption in single crystals and at temperature below 90°K.[3] We knew their result by a private communication*, when our repeated measurements had been finished with newly obtained crystals** and our preceding report[4] prepared. Bleaney and Bowers concluded that all their results can be well fitted to the effective spin-Hamiltonian

$$\mathcal{H}=\tilde{g}\beta\vec{H}\vec{S}+DS_z^2+E(S_x^2-S_y^2) \qquad (1)$$

with two paramagnetic units in unit cell each having an effective spin $S=1$ and with the parameters $\tilde{g}$, D, and E as listed in Table I. This was explained with an assumption of strong exchange forces between ions belonging to the same pair. They also observed that the absorption line shows a curious structure in some directions. This could be also explained as a hyperfine structure caused by two nuclei of the interacting copper atoms, which supports the above-mentioned assumption of coupled atoms.

Table I. Proper values to be given as parameters appeared in the spin-Hamiltonian (Eq. (1)) in order to cover the experimental results as a whole.

	Our results	Bleaney and Bowers
g_z	$2.34_4 \pm 0.01$	2.42 ± 0.03
g_x	$2.05_3 \pm 0.005$	2.08 ± 0.03
g_y	$2.09_3 \pm 0.005$	2.08 ± 0.03
$D_{(cm^{-1})}$	$0.34_5 \pm 0.005$	0.34 ± 0.03
$E_{(cm^{-1})}$	0.005 ± 0.003	0.01 ± 0.005

Guha[6] discovered previously an anomaly in the static susceptibility of this salt. In ordinary copper salts, static susceptibility χ agrees well with the Curie-Weiss law

* The authors wish to thank them for their information on hydration number of this salt.

** The authors are indebted to Prof. Nakanishi, Department of Chemistry, Ochanomizu University, for carrying out some of the chemical analysis of specimens.

$$\chi=\frac{C}{T+\Theta} \qquad (2)$$

with Θ of several degrees. So it increases monotonically with decreasing temperature around the region of room temperature. In copper acetate, however, it shows a broad maximum at about room temperature, 265°K, and falls down rapidly with decreasing temperature. This was explained by Bleaney and Bowers with a diamagnetic singlet level ($S=0$) which lies lower than the paramagnetic triplet level ($S=1$) by an energy amount of 450°K or 315 cm^{-1}. This level scheme is also derivable from the assumption of couples of strongly interacting ions.

Recently Foëx *et al*[7] repeated susceptibility measurements of this crystal paying attentions to the preparation of specimens and confirmed the existence of maximum susceptibility at about 265°K as reported by Guha previously. At the lower temperature side, however, their results deviates from Guha's which they ascribed to some paramagnetic impurities in the specimens used by the latter author.

§ 2. On Samples

Our sample crystals were prepared as follows. The pure powder of copper acetate (not basic) is solved in distilled water added with suitable amount of acetic acid. This solution of about 500 cc is kept in a glass beaker and put under natural vaporization of water. After several days many little single crystals are obtained. After filtration, some of them are suspended as seed crystals in the filtered solution which is then put in a thermostat. After some weeks, they grow up to the crystals having linear dimension of $10 \sim 15$ mm. They are of dark green and monoclinic with parameters[8] of $a:b:c=1.5320:1:0.8108$; $\beta=116°26'$.

In our case, the number of prepared crystals being of order 500, all the samples that were examined are twins, having the $(20\bar{1})$ plane as twinning plane. This was pointed out by Kiriyama at Osaka University who kindly examined some of our samples and informed that all the specimens examined have twin structure. Then, he and his co-laboratours started to analyse this crystal by the x-ray method to determine its atomic constructions. The unit cell parameters were obtained as $a=13.10$Å, $b=8.56$Å and $c=13.88$Å, using Groth's data of $\beta=116°26'$, so that the twinning plane is the $(10\bar{1})$ plane with respect to these axes.*

The specimens used for our measurements were ground out from

* On their way of analysis, however, it was reported by Bleaney et al[6] that the x-ray analysis of this crystal was almost finished in England, so they gave up their plan.

some of crystals having volumes greater than about 0.5 cc, whenever a plane was desired. At least two samples were prepared to avoid errors caused by misgrinding and more than for detailed measurements. The maximum error in angle from misgrinding ranged to $2^\circ \sim 4^\circ$ according to the sorts of planes desired. This error in angle from misgrinding could be reduced by optical measurements of the external form after the specimen was mounted with polystyrene cement at the rotatable mount of the cavity. After this adjustment, error in angle becomes less than about 1°.

§ 3. Experimental Apparatus

At first, the resonance absorption was observed at about 16 mm wavelength. Afterwards, observations at other wavelengths, *i.e.* 8, 11, and 30 mm, were also performed. The systems of microwave circuit are the same for the three channels of shorter wavelengths, the microwave power which transmits through attenuators and the cavity for measurement is detected by a crystal diode and its rectified current is measured by a galvanometer.

The *rf*-powers of $\lambda=8$, 11, and 16 mm were obtained by the crystal multiplier method already described[9], using $3.0 \sim 3.2$ cm wave as their foundamental which was fed by a 2K25-type klystron. The *dc* voltages, V_{cav} and V_{rep}, for the klystron were supplied by electronically stabilized power sources whose stabilization factor[10] $S=\left(\frac{\Delta V_{ac}}{V_{ac}}\right)\Big/\left(\frac{\Delta V_{op}}{V_{op}}\right)$ was measured to be −800 and −130 respectively. Here V_{ac} means the line voltage, V_{op} the stabilized out-put voltage and Δ the variation in them. Ten percent drop in the *ac*-line voltage V_{ac} causes a variation of about one part in thousands of 3 cm power level and of about 0.3 Mc in its frequency. Within half an hour after the voltages were supplied, the frequency shift is not negligible for our purpose which may be attributed mainly to the thermal expansion of klystron cavity. So, measurements must be begun with at least half an hour's wait after the proper voltages are supplied. By protecting the klystron from the convection of air by means of a thermal shield, a fairly adequate constancy in power level and in frequency can be maintained within few runs of measurement for which about half an hour is needed. This constancy is severely demanded as far as the absorption intensity is concerned, which will be discussed elsewhere[11]. The power intensity of these higher harmonics decreases with their increasing order[17]. It was sufficient in both cases of 11 mm and 16 mm measurements. It was fairly adequate for 8 mm case, since the absorption coefficient of the usual line increases with increasing frequency, except the case of the line appearing at the lower most field and having decreasing intensity when the measuring frequency

is increased. The dip of galvanometer reading at the resonance magnetic field of single peak at $\lambda=16$ mm was about 4 percent of the initial deflection. The galvanometer dip for the weakest line at 8 mm was about $5 \sim 10$ times of fluctuation. This fluctuation comes mainly, in our case, from that of the multiplier crystal and it usually diminishes within some days after the multiplier crystal has been set up.

The cavities for measurement are of rectangular type excited in the H_{101} mode, (in some cases in H_{10^2}). As an example, cross-sectional view of the resonant cavity used at the "10 mm channel" is shown in

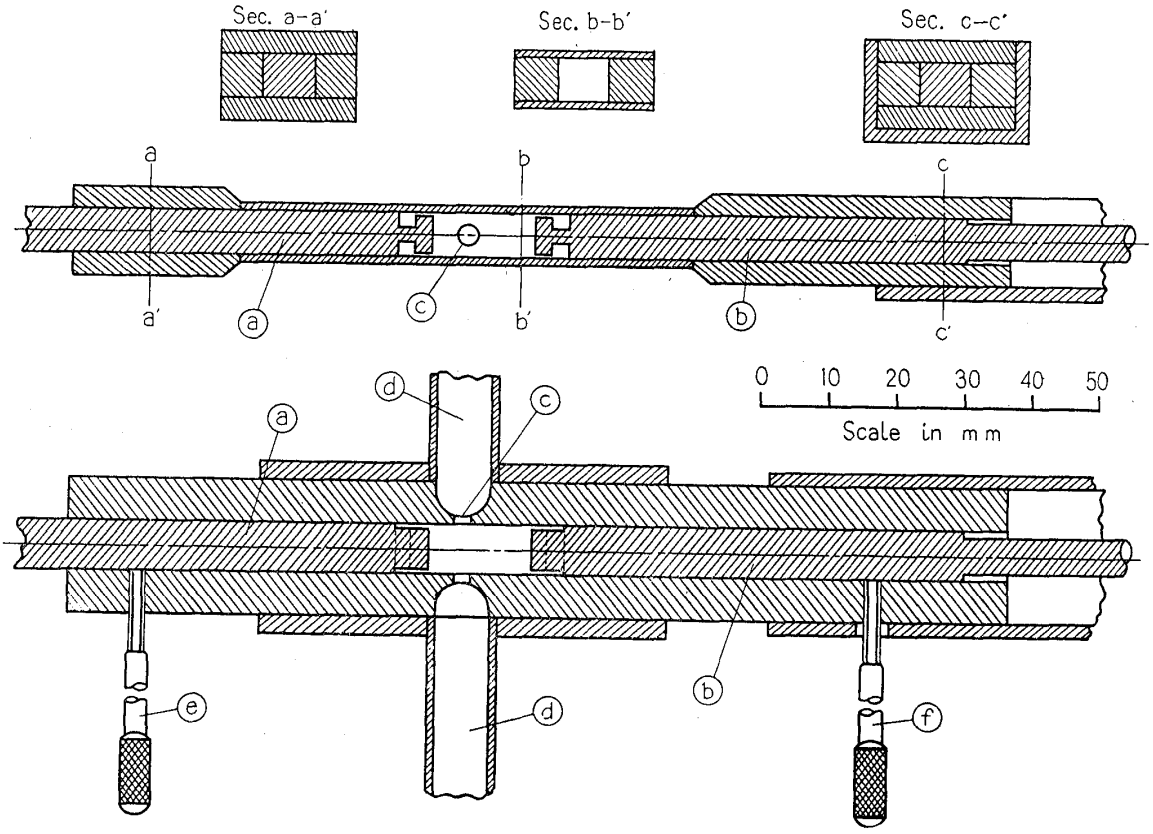

Fig. 1. Cross-sectional view of cavity resonator used at the "10 mm channel".

a) Sample piston. (Details of mechanism for sample rotation are neglected. See Fig. 2 (a))
b) Tuning plunger. (Mechanisms of varnier tuner are neglected. See Fig. 2 (b))
c) Coupling window.
d) Wave-guides.
e) Screw for setting the sample piston (a).
f) Screw for rough setting of the tuning plunger (b).

Fig. 1. Detailed construction of its two main parts, sample piston with rotatable crystal mount and tuning plunger with varnier tuner, are shown in Fig. 2. Other three cavities used at the other channel have dimensions listed in Table II. For channels other than "x-band" or "32 mm channel", cross-section of sample cavity is nearly squar-shaped,

because the disc-shaped sample crystal on the rotatable mount has a larger filling factor for this type of measuring cavity. It is specially adequate for the measurements on the same sample at different frequencies. In the cavities of 16- and 8 mm-channel, dimension A of Fig. 2(b) is greater than B, to avoid the cross-mixing of the higher-mode resonances.

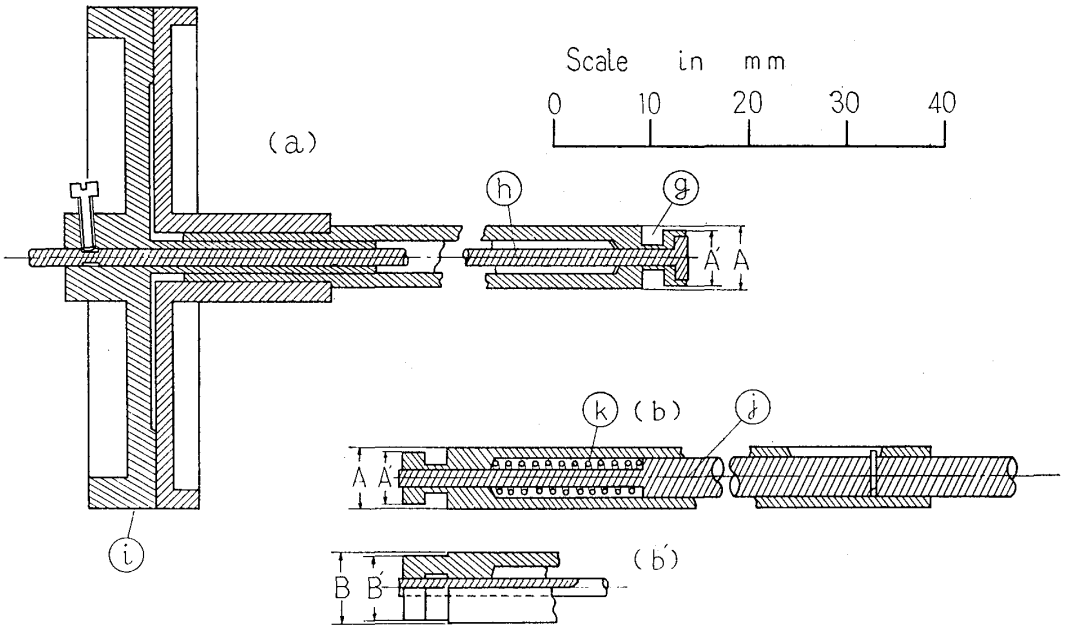

Fig. 2. Details of (a) sample piston and (b) tuning plunger with dimensions at "10 mm channel".

g) Quarter wave choke section.
h) Rotatable mount for sample crystal.
i) Handle for sample rotation having 360° angle indication with varnier scale.
j) Tuning cylinder as a varnier tuner.
k) Phospher bronze spring.

Table II. Dimensions (in mm) of cavity resonators for measurement. (For notations of A, etc. see Fig. 2 (b)).

Channel. (mm)	A	A'	B	B'
32	10.2	9.2	20.0	19.2
16	10.0	9.6	8.95	8.5
10	6.3	5.85	7.4	6.8
8	5.0	4.6	4.4	4.0

Static magnetic field is supplied by an electromagnet. It was calibrated by proton resonance method. After each several runs and after any adjustment of voltages supplied for the klystron, resonance measurement for the free radical *DPPH* was performed which was used as the marker[16] for $g=2.00$.

§ 4. Results

A. Experimental procedures

A plane is ground out at some of the single crystals to obtain the *ac*-plane by their external forms. The crystal is then attached to the rotatable mount of the measuring cavity by its polished plane. So the magnetostatic field H is rotated in this ground *ac*-plane. Fig. 4 is an example of absorption curves which was observed at $\lambda=16.5_8$ mm and when the static magnetic field was set at $\varphi=34°$, where angle φ means the direction of static field measured from the *c*-axis towards the *a*-axis, as shown in Fig. 3. Here three peaks can be seen in Fig. 4, though one appearing at the lower most magnetic field has a very weak absorption intensity around this direction of H. Since it is so weak at $\lambda=8$ mm case that it almost escapes in the fluctuations in our spectrometer. Two of them appearing at the upper magnetic field vary their resonance value when the direction of H is rotated in the *ac*-plane. In

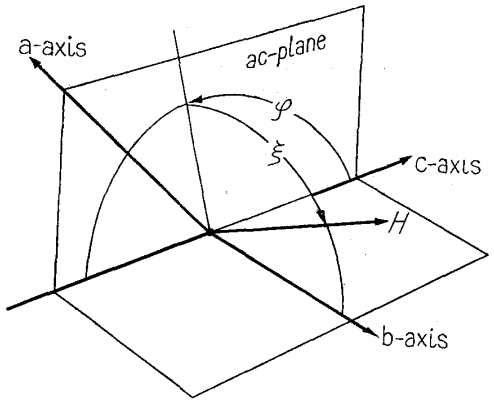

Fig. 3. Notation of angles used in the text to indicate the direction of the static magnetic field H.

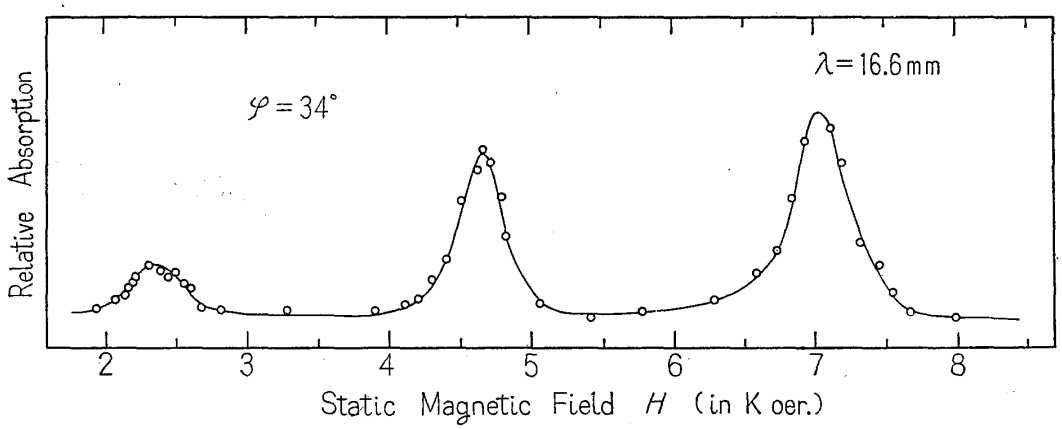

Fig. 4. Absorption peaks of copper acetate monohydrate measured in its *ac*-plane and at $\lambda=16.5_8$ mm.

Fig. 5 the values of resonant magnetic field at $\lambda=7.83$ mm are plotted as functions of the angle φ. These two peaks are called as line (a) and (b) in this article. The resonance magnetic field H for these lines has its maximum and minimum at $\varphi=\psi$ and $\psi+90°$ respectively. From

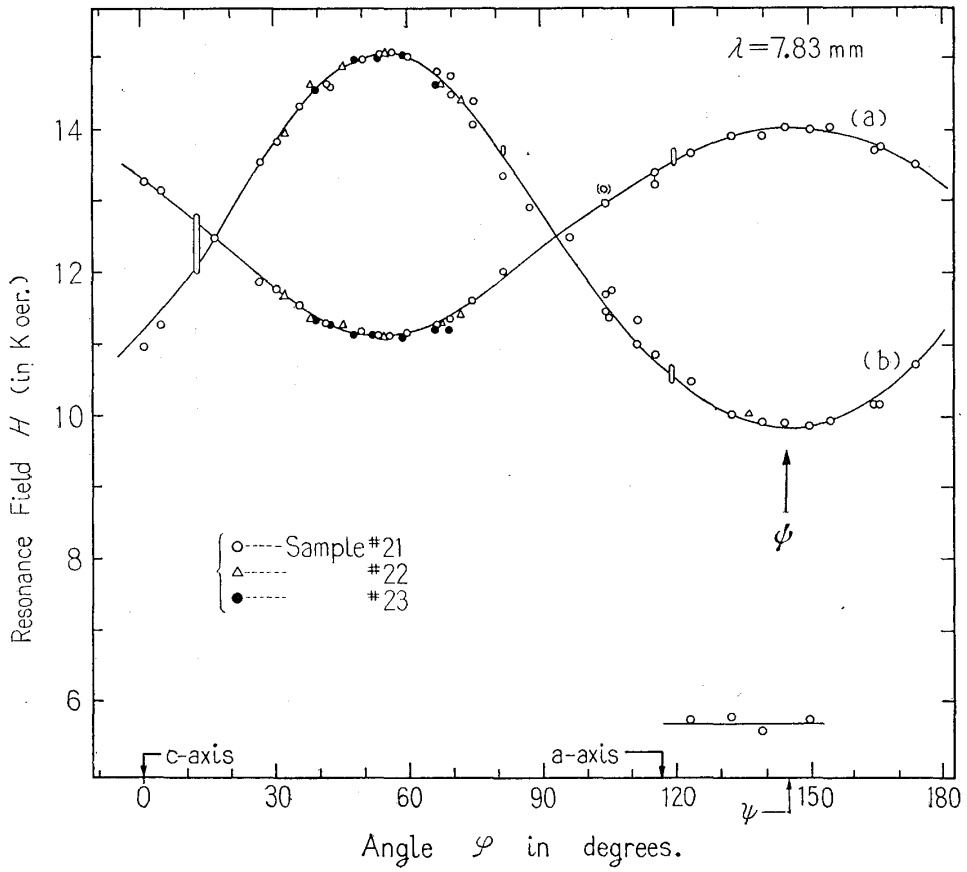

Fig. 5. Magnetic field at absorption peaks plotted as functions of magnetic field direction in the ac-plane of copper acetate monodydrate measured at $\lambda=7.8_3$ mm.

our experiments, angle ψ was determined to be $-34.5°\pm1.5°$. Strictly speaking, the angle φ at which the line (a) reaches to its highest magnetic field does not necessarily agree with the angle where the line (b) shows its lowest resonance field. Then it results an uncertainty of 1.5° in determination of angle ψ.

Then other single crystals are cut to obtain the plane perpendicular to the ac-plane at $\varphi=-34.5°$. In this plane the line (a) splits into two lines (a, 1) and (a, 2), and the line (b) behaves as well as (a), as shown in Fig. 6. Results obtained at $\lambda=10$ and 15 mm are shown in Figs. 7 and 8. The direction of H in this plane is expressed by an angle ξ measured from the ac-plane, as shown in Fig. 3. The line (a, 1) and

(b, 1) show their extreme value at $\xi=\alpha$ ($\alpha \leqq 90°$), which is experimentally determined to be $33° \pm 1°$. Fig. 9 is an example of results of resonance absorption, decrease in galvanometer reading, observed at $\xi \fallingdotseq 35°$ *i.e.* the direction of static field H makes an angle of about 2°

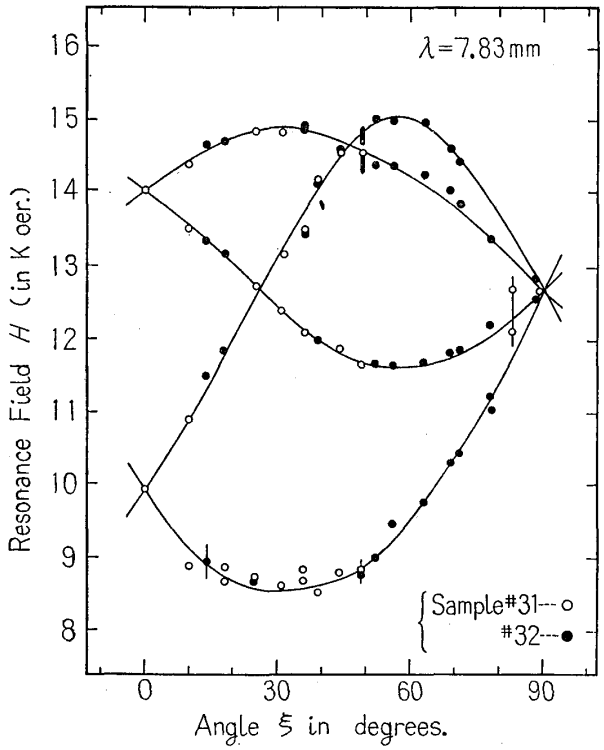

Fig. 6. Resonance peaks of copper acetate monohydrate plotted against the direction on static magnetic field observed at $\lambda=7.83$ mm in its zz-plane *i.e.* the plane containing z-axes of two inequivalent magnetic units.

with the axis of the dominant crystalline field of one of the magnetic complexes. In this case, again, the angle ξ at which the line (a, 1) comes to its maximum does not coincide experimentally with that the minimum of the line (b, 1). This is mainly responsible for the uncertainty in determinantion of the angle α. The angles thus determined are listed in Table III. By $\varphi=\psi$ and $\xi=\pm\alpha$, two directions are given, each of which means the direction of the predominant tetragonal axis of crystalline field. This direction is here labeled as z-axis. Axis x is taken perpendicular to the z-axis within the plane containing two z-axes and y perpendicular to both z-axes. So the y-axis lies essentially in the ac-plane.

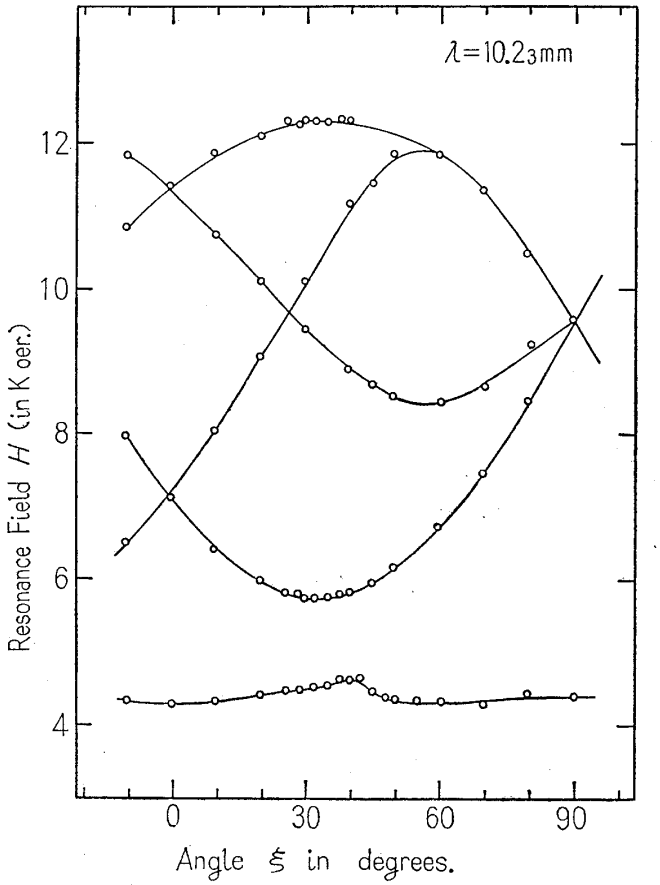

Fig. 7. Resonance peaks of copper acetate monohydrate plotted against the direction of static magnetic field observed at $\lambda=10.23$ mm in its zz-plane *i.e.* the plane which contains z-axes of two inequivalent magnetic units.

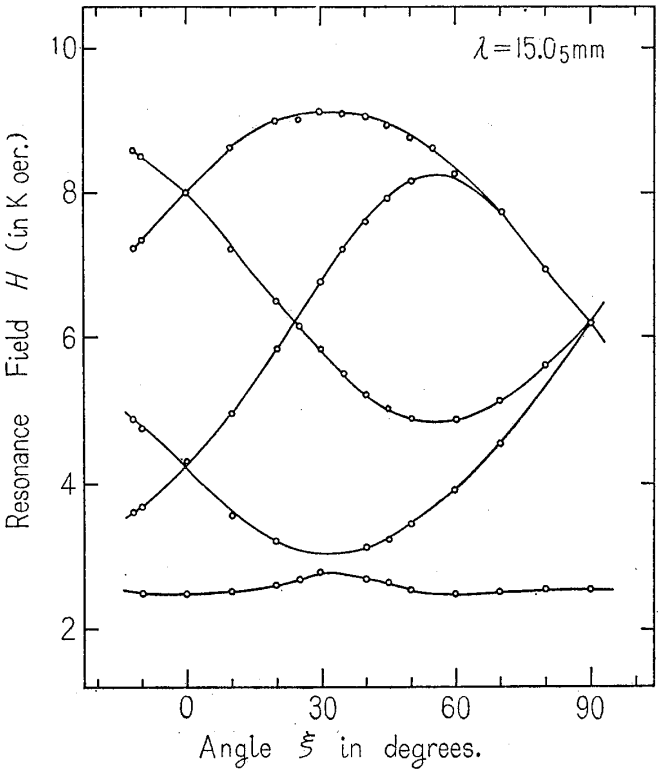

Fig. 8. Resonance peaks of copper acetate monohydrate plotted against the direction of static magnetic field observed at $\lambda=15.05$ mm in its zz-plane *i.e.* the plane containing z-axes of two inequivalent magnetic units.

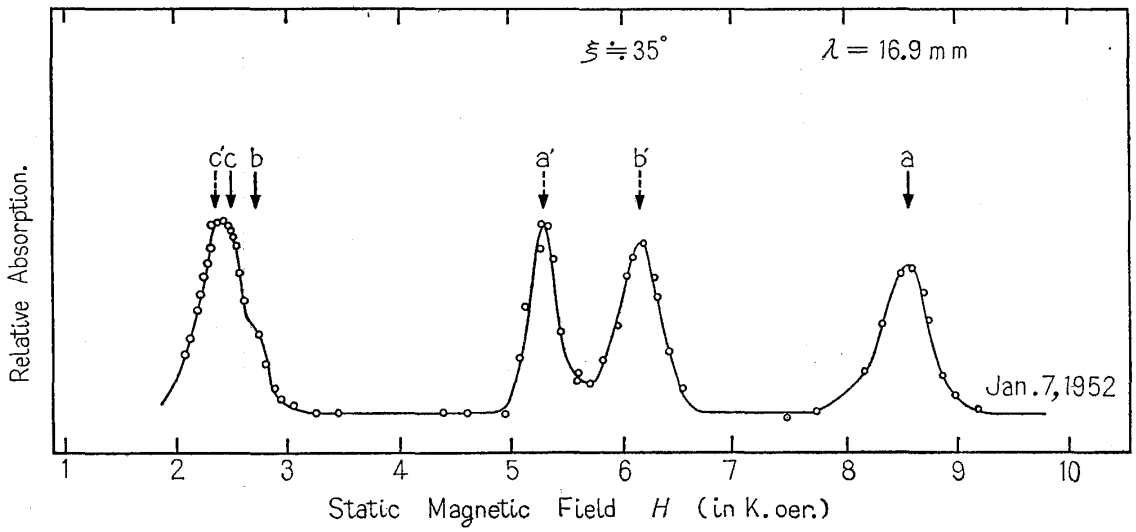

Fig. 9. Decrease in galvanometer reading showing peaks of resonance absorption observed at room temperature, the static magnetic field being applied nearly parallel to the z-axis of one of the magnetic units. Peaks a, b, and c are originated from this unit and a′, b′, and c′ from the other unit, z-axis of which makes an angle of about 2α from the static magnetic field H.

Table III. Angles indicating the direction of the predominant crystalline field referred to the crystallographic axes.

Author	This report	Bleaney et al[2]	van Niekerk et al[3]	Guha[5]
Method	P.R.A.	P.R.A.	X-ray	Static χ
ψ (in deg.)	-34.5 ± 1.5	-33	-32.7	$+23$[b]
			(-34.1)[a]	
α (in deg.)	33 ± 1	33	34.6	

Remarks: a) Mean value for a twinning crystal.

b) In Guha's report, it is supposed that the $(20\bar{1})$ plane (the twinning plane) is mistaken as the c-plane.

B. Eigenvalues of the Hamiltonian and Experimental Resonance Fields

The Hamiltonian (1) can be rigorously solved at the directions of the three principal axes. In the case when H is applied at the z-direction, the eigenvalues are

$$\left.\begin{aligned} W_{\pm} &= D \pm \sqrt{E^2 + g_z^2 \beta^2 H^2} \\ W_0 &= 0 . \end{aligned}\right\} \qquad (3)$$

Here g_z is the z-component of $\tilde{g}$ tensor and subscripts in W mean their quantum number M.

When the applied field is so weak that the Zeeman term is comparable with the crystalline field perturbation, the quantization of the system is not perfect. In the directions of principal axes, however, the three states do not commute themselves but remain their pure character at any field strength of H. In the general direction, subscripts $\pm$ and 0 have the meaning that the quantum number M of the corresponding states becomes ±1 and 0 respectively, when the applied

magnetic field H becomes so strong that the splitting caused by the crystalline field is negligible compared with its Zeeman term.

In the case when H is in the x- or y- direction,

$$\left.\begin{aligned} W_{\pm}&=\tfrac{1}{2}(3\delta E-D)\pm\sqrt{\tfrac{1}{4}(D+\delta E)^2+g_{x,y}^2\beta^2H^2} \\ W_0&=0\,. \end{aligned}\right\} \qquad (4)$$

where δ means $+1$ in x-direction and -1 in y-direction. In Figs. 10 and 11, differences between these eigenvalues are shown as functions of applied field H using the parameters listed in Table I, where $\Delta W_{+\to 0}$ means $W_+ - W_0$ etc. Besides our results at room temperature, results

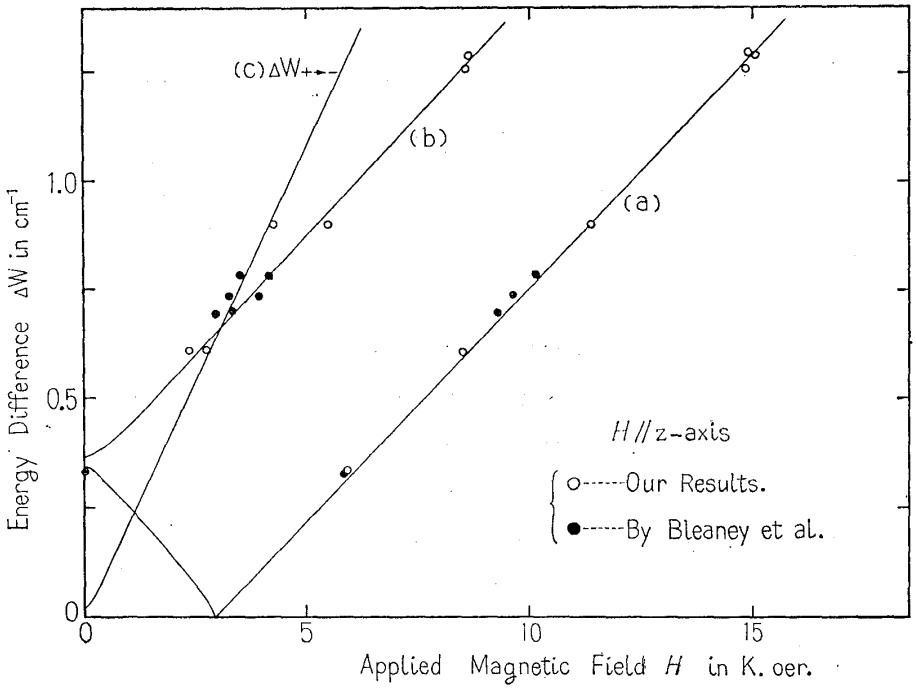

Fig. 10. Energy differences between the levels as functions of the static magnetic field H applied in the z-direction. Solid lines are calculated from Eq. (3) with parameters listed in table I, whereas points indicate the experimental results.

by Bleaney and Bowers[6] at 90°K are also plotted in the figures. The calculated curves can be best fitted to our experimental values when the parameters appearing in Eq. (1) are chosen as listed in Table I. In order to see angular variation of resonance spectrum, the perturbation treatment was carried out at the arbiturary direction of applied field H, assuming the Zeeman energy is sufficiently greater than the crystalline field interactions.

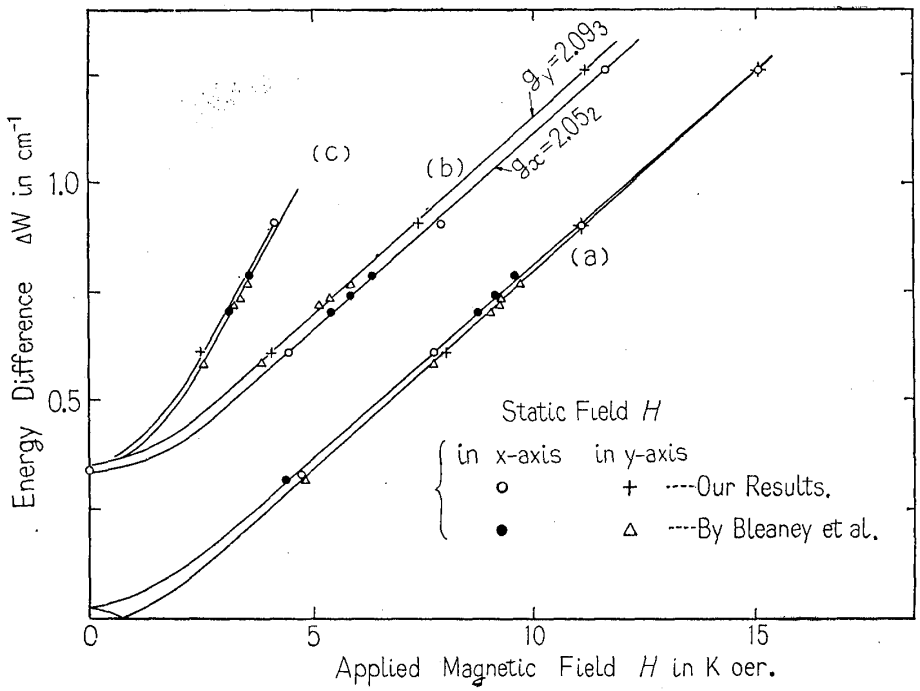

Fig. 11. Energy differences between the levels as functions of the static magnetic field H applied in the x- and y-directions. Solid lines are calculated from Eq. (4) with parameters listed in table I, whereas points indicate the experimental results.

$$\left.\begin{aligned} \Delta W_{+\to 0} &= g\beta H + D(3p^2\cos^2\theta - 1)/2 \\ &\quad + 3E(q^2\sin^2\theta)/2 + \Delta W_{(2)} \\ \Delta W_{0\to -} &= g\beta H - D(3p^2\cos^2\theta - 1)/2 \\ &\quad - 3E(q^2\sin^2\theta)/2 + \Delta W_{(2)} \\ \Delta W_{+\to -} &= 2g\beta H + 2\Delta W_{(2)} \end{aligned}\right\} \qquad (5)$$

where

$$p = g_{//}/g \quad \text{and} \quad q = g_{\perp}/g \qquad (6)$$

Here θ means the angle between the applied magnetic field and the z-axis of crystalline field, g the component of $\tilde{g}$ tensor along the static field H, and $\Delta W_{(2)}$ the term from the second order perturbation,

$$\Delta W_{(2)} = \frac{(D+E)^2 q^2 \sin^2\theta\{4p^2\cos^2\theta + q^2\sin^2\theta\}}{8H_0} \quad \text{(oer.)} \qquad (7)$$

where H_0 means the resonance field for the free electron. This correction term is estimated to reach to its maximum value $\sim 5D^2/32H_0$ at $\theta \simeq 45°$. It is negligible when $H \geqq 10$ K oer.

Transition occurs when the applied field H makes ΔW in Eq. (5) equal to $h\nu$. We call this value of H as $H_{+\to 0}$, $H_{0\to -}$ and $H_{+\to -}$ which give the line (a), (b) and (c) respectively.

In order to obtain the more precise values of the parameters shown

in Table II, the measurements were repeated in directions around the principal axes. The experimental procedures used to minimize errors in determining peak positions in these principal directions has been described elsewhere[12] in case of $Cu(NH_3)_4 \cdot SO_4 \cdot H_2O$. The results plotted in Figs. 10 and 11 were obtained with this manner.

C. Line Width

In our experiments at room temperature, the full line width observed at the z-direction is as follows. At $\lambda=8$ and 16 mm, it is about 400 oer. for the line of $|\Delta M|=1$ appearing at the highest magnetic field and about 300 oer. for the other $|\Delta M|=1$ transition appearing at the lower magnetic field. These values are somewhat greater than the width of Bleaney's measurements at 90°K. Moreover, in our case at room temperature, any hyperfine structure can be observed, even by the modulation method. These disagreements may be ascribed either to the dipole-dipole interaction or to the spinlattice relaxation.

The dipole contribution to the width[13] is estimated to be about 385 oer assuming that all the pairs of copper ions are in their paramagnetic triplet state and distributed with an average distance of 7.30 Å deduced from the volume of unit cell. At a given temperature, some of the pairs of copper ions go down to their ground state which is diamagnetic singlet. This situation can be treated as a reduction in the number of the paramagnetic carriers in unit cell such as dilution in diamagnetic salts. The dipole width of Van Vleck[13] is proportional to the sqare root of this reduction at about our concentration, while it is proportional to the reduction only at very low concentration[19]. So the dipole width at 90°K and 300°K are estimated to be 31 oer. and 165 oer. respectively, using $J=315\,cm^{-1}$ as the level splitting obtained from the susceptivility measurements. The dipole width at room temperature exceeds the hfs constant A, 80 oer, in our crystal. This is one of the possible explanations for the disappearance of hfs at room temperature. Since the assumption of cubic lattice of pairs gives the minimum, the real lattice is considered to give slightly larger dipole width, c.a., 200 oer. Taking account of the contribution from the unresolved hfs as the second moment, the results of linewidth in our measurements are reasonable ones.

§ 5. Discussions

A. Atomic Structure of the Crystal

After we finished our experimental works, we knew that van Niekerk and Schoening[14] have reported the x-ray study of this crystal. They treat this crystal as a new type of copper complex, that is $Cu_2 \cdot$

$(CH_3COO)_4 \cdot 2H_2O_2$. By their result, the unit cell has dimensions of

$$a=13.15\text{Å}, \quad b=8.52\text{Å}, \quad c=13.90\text{Å} \quad \text{and} \quad \beta=117^\circ\ 0'$$

which contains 4 binuclear molecules described above. The structure of this molecule $Cu_2(CH_3COO)_4 \cdot 2H_2O$ is shown (schematically) in Fig. 12 by which we can see a direct Cu–Cu contact at an interval of 2.64Å. This atomic construction gives rise to isolated pairs of cupric ions which cause an anomalous $S=1$ character in this crystal.

The z-direction in our Hamiltonian (1) may correspond to the line ζ. Here ζ means the line joining the two copper ions in a pair. From the view-point of microwave resonance, our attention is confined only to its relative orientations reffered to the crystalline axes, so there are two

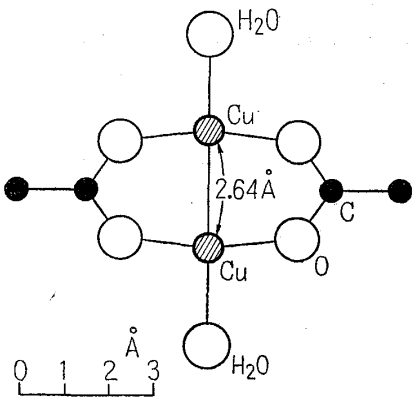

Fig. 12. Side-view of a magnetic complex, $Cu_2\{CH_3COO\}_4 \cdot 2H_2O$, in crystal of copper acetate monohydrate, where positions of hydrogen are omitted, after van Niekerk and Schoening.[14]

inequivalent ζ-directions derivable from the x-ray analysis, which are in symmetry directions with the ac-plane. From the x-ray data, the projection of these two lines in the ac-plane makes an angle of $-32^\circ 46'$ with the c-axis. In twinning crystals, however, besides the ζ-line from the normal part of the crystal, there is another sort of ζ-line from the twinning part which is called as ζ'-line. The projection of line ζ' makes an angle of $-35^\circ 28'$ with the c-axis. Two adjacent peaks may be expected in these twinning crystals, since the z-directions for the two parts of crystal are slightly different (by 2.7°). However, the estimated difference between the two peaks becomes the maximum of 230 oer. at about $\theta \approx 45^\circ$ and at the three principal axes it is only $10 \sim 20$ oer. The existence of the twinning part only makes the width of resonance line somewhat broader. So, in twinning samples, the observed peak in resonance absorption which can not been resolved into peaks may give a mean value $-34^\circ 07'$ of these angles. This is also the angle between the normal of the twinning plane and the c-axis and is in a fair agreement with our result in paramagnetic absorption, since the latter is -34.5°

$\pm 1.5°$ as listed in Table III.

On the other hand, the line ζ, from the x-ray data, makes an angle of 34°43′ with the *ac*-plane, while our experiments give an angle of $\alpha=33°$.

B. Exchange Energy

Bleaney *et al* introduced the effective spin-Hamiltonian (1) from a Hamiltonian

$$\mathscr{H}=X_1+X_2-J\vec{S}_1\vec{S}_2+\lambda(\vec{L}_1\vec{S}_1+\vec{L}_2\vec{S}_2)+\beta\vec{H}(\overrightarrow{L_1+2S_1}+\overrightarrow{L_2+2S_2}) \quad (8)$$

where subscripts 1, 2 refer to the two ions: X denoted the crystalline electric field interaction, J is the exchange integral and λ the spin-orbit coupling coefficient. The exchange energy J gives rise to remove the ground states to a singlet and a triplet which lies higher as J than the singlet. This triplet is further split by the interplay of exchange coupling and the crystalline field into a doublet and a singlet, energy difference of which is a function of the direction of the static magnetic field relative to the crystalline axes. From this level scheme, the parameter D appeared in the effective Hamiltonian (1) is introduced as

$$D=\frac{\lambda^2}{2}\left[\frac{J_2}{\Delta_2^2}-\frac{4J_1}{\Delta_1^2}\right] \quad (9)$$

or

$$D=-\frac{1}{8}\left[\frac{J_1}{4}(g_{//}-2)^2-J_2(g_\perp-2)^2\right] \quad (10)$$

where Δ_1 and Δ_2 are energy differences between the ground state and the first and the second higher orbital level. J_1 and J_2 means the exchange energies corresponding to Δ_1 and Δ_2, respectively. If we assume $J_1=J_2$, Eq. (10) gives

$$J_1=\frac{-32D}{[(g_{//}-2)^2-4(g_\perp-2)^2]} \quad (11)$$

By this equation, results of our experiments at room temperature give $J_1=110\pm20\ \mathrm{cm}^{-1}$ whereas the results at 90°K by Bleaney and Bowers give $J_1=75\pm10\ \mathrm{cm}^{-1}$.

Exchange energy between two directly interacting atoms is considered to be dependent on their distance R by a relation[18]

$$J\propto\exp(-\Delta R/0.345) \quad (12)$$

where ΔR means the change in Å. To estimate ΔR of the Cu–Cu distance from the thermal origin, a coefficient of linear thermal expansion

4×10^{-5}/deg is assumed to our crystal, being usual value for hydrated salts. Exchange energy J at 90°K is then estimated to be 1.06 times as large as that at 290°K, whereas experimental results gives a slightly larger value, within their errors, than that estimated.

In order to account for the Guha's results on the temperature dependence of paramagnetic susceptibility of this crystal, Bleaney and Bowers introduced an assumption that the exchange energy J at ground states varied from 315 cm^{-1} at room temperature to 255 cm^{-1} at 90°K. However, the more recent results on susceptibility by Foëx *et al* can be well explained by a single value of J.

§ 6. Acknowledgements

The authors wish to express their sincere thanks to Professor Hiroo Kumagai for his continuous guidance and to Drs. K. Ôno and I. Hayashi for their helps in measurements at 3 cm region. They also wish to thank Profs. K. Kambe and R. Kiriyama for their valuable discussions and suggestions, to Prof. M. Nakanishi for chemical analysis, to Mr. H. Osafune of the Nihon Electric Co., Ltd. for a part of silicon wafers and to Prof. R. D. Myers for the marker radical.

References

1) K. Kambe (unpublished work). Report given at the session on magnetism of the Physical Society of Japan held at Sendai (May, 1952).
2) F. W. Lancaster and W. Gordy: Jour. Chem. Phys. **19** (1951) 1181.
3) B. Bleaney and K. D. Bowers: Phil. Mag. **43** (1952) 372.
4) H. Kumagai, H. Abe, and J. Shimada: Phys. Rev. **87** (1952) 385.
5) B. Bleaney and K. D. Bowers: Proc. Roy. Soc. **A214** (1952) 451.
6) B. C. Guha: Proc. Roy. Soc. **A206** (1951) 353.
7) G. Foëx, T. Karantassis, and N. Perakis: Comp. rendus **237** (1953) 982.
8) P. Groth: *Chemische Kristallographie* (Leipzig, 1910) vol. **3**, p. 66.
9) H. Abe, K. Ôno, I. Hayashi, J. Shimada, and K. Iwanaga: Jour. Phys. Soc. Japan: **9** (1954) 814.
10) W. C. Elmore and M. Sands: *Electronics*. National Nuclear Energy Series, McGrow-Hill Book Co. Inc. 1949, p. 364.
11) H. Abe, T. Negishi and Y. Obata: to be published.
12) H. Abe and K. Ôno: Jour. Phys. Soc. Japan. **11** (1956) 947.
13) J. H. van Vleck: Phys. Rev. **74** (1948) 1168.
14) J. N. van Niekerk and F. R. L. Schoening: Acta Cryst. **6** (1953) 227.
15) N. Perakis, A. Serres, and T. Karantassis: Jour. Phys. et Rad. **17** (1956) 134.
16) B. Bleaney and D. J. E. Ingram: Proc. Roy. Soc. **A205** (1951) 336.
17) C. M. Johnson, D. M. Slager, and D. D. King: Rev. Sci. Inst. **25** (1954) 213.
18) M. Born and J. E. Mayer: Zeit. Phys. **75** (1932) 1.
19) C. Kittel and E. Abrahams: Phys. Rev. **90** (1953) 238.

(Received April 30, 1957)